Clays and Clay Minerals, Vol. 58, No. 4, 451–461, 2010.

MINERALOGICAL, CHEMICAL, AND PHYSICAL CHARACTERIZATION OF SYNTHETIC Al-SUBSTITUTED MAGHEMITES (γ-$Fe_{2-x}Al_xO_3$)

MARCELO A. BATISTA[1,*], ANTONIO C. S. DA COSTA[1], JERRY M. BIGHAM[2], HENRIQUE DE SANTANA[3], DIMAS A. M. ZAIA[3], AND IVAN G. DE SOUZA JUNIOR[1]

[1] Universidade Estadual de Maringá, UEM, Departamento de Agronomia, Av. Colombo 5790, 87020-900, Maringá, PR, Brazil
[2] The Ohio State University, School of Environment and Natural Resources, 2021 Coffey Road, 210 Kottman Hall, 43210-1085 Columbus, OH, USA
[3] Universidade Estadual de Londrina, UEL, Departamento de Quèmica, 86051-990, Londrina, PR, Brazil

Abstract—Maghemite (γ-Fe_2O_3) is a ferrimagnetic Fe oxide commonly found in tropical and subtropical soils, especially in the topsoil where it is usually a product of burning. Isomorphic substitution (IS) of the Fe in maghemite by different metals (mainly Al^{3+}) can modify its mineralogical and chemical attributes, and these modifications may be important to understanding the formation and properties of this mineral in soils and sediments. The objective of this work was to evaluate the crystallochemical alterations of synthetic, Al-substituted maghemites prepared by the precipitation of magnetites from alkaline aqueous media containing $FeSO_4 \cdot 7H_2O$ with increasing amounts of $Al_2(SO_4)_3 \cdot 7H_2O$ to obtain hypothetical Al^{3+} for Fe^{3+} substitutions ranging from 0.0 to 40.0 mol %. The Al-substituted magnetites were washed and dried, and then heated to 250ºC for 4 h to form yellowish red maghemites that were characterized by total chemical analysis, X-ray diffraction, specific surface area (SSA), mass-specific magnetic susceptibility, infrared spectroscopy, transmission electronic microscopy, and color. Increasing Al^{3+} substitution to an experimental maximum of 15.9 mol % decreased both the a_0 dimension of the cubic unit cell ($a_0 = 0.8339 - 396.157 \times 10^{-6}$ Al, $r^2 = 0.99$) and the mean crystallite dimension (MCD = 76.4 − 3.15Al, $r^2 = 0.79$) of the maghemites. With the decrease in MCD came a more yellowish color, an increase in SSA, and a decrease in crystallinity as measured through extraction of the samples with acid ammonium oxalate. The mass-specific magnetic susceptibility of the maghemites increased with Al^{3+} substitution up to 5.3 mol % and then decreased with further replacement of Fe by Al. Solid-phase aluminum in excess of 16 mol % substitution appeared to occur as a separate, poorly crystalline phase that was X-ray amorphous.

Key Words—Fe Oxides, Isomorphic Substitution, Mass Specific Magnetic Susceptibility, Specific Surface Area, X-ray Diffraction.

INTRODUCTION

Iron oxides and oxyhydroxides are important minerals in many highly weathered tropical soils and may strongly influence their chemical, mineralogical, or pedological behavior and influence agricultural management practices (Wiriyakitnateekul *et al.*, 2007). Iron oxides in soils vary by mineral species, crystal size, structural order, and composition, and variations in these properties may reflect differences in the environmental conditions prevailing during pedogenesis (Schwertmann and Taylor, 1989). As soil Fe oxides generally form by precipitation from pore waters, foreign ions and molecules present in the soil solution may be incorporated into the Fe oxide structures or adsorbed to particle surfaces, and both processes may affect crystal growth (Schulze and Schwertmann, 1984).

Soil formation usually results in an increase in magnetic susceptibility (Cabello *et al.*, 2009). In soils and sediments, magnetite (Fe_3O_4) and maghemite (γ-Fe_2O_3) are common ferrimagnetic oxides (Cornell and Schwertmann, 1996) and have been investigated extensively because of their important applications in industry (Campbell *et al.*, 2000) and the environment (Benjamin *et al.*, 1982; Zachara *et al.*, 2004; He and Traina, 2007). Relatively little is known about their properties in soils, however. Naturally occurring magnetites and maghemites are frequently intergrown with other minerals or form highly stable aggregates, making their separation and purification from soils and sediments rather difficult (Cornell and Schwertmann, 1996). For example, the clay fractions of many soils developed from volcanic rocks in southern Brazil exhibit spontaneous magnetization caused by the presence of fine-grained maghemites, but few attempts have been made to quantify or characterize this important soil component (Costa *et al.*, 1999).

Maghemite (γ-Fe_2O_3 or $Fe_{8/3}\square_{1/3}O_4$) has a spinel structure with Fe^{3+} distributed among tetrahedral (A) and octahedral (B) sites. The number of B sites is twice that of the A sites. The actual distribution of vacancies ($\square$) is still controversial, and they are reported to occur exclusively in B sites, or in both A and B sites (Armstrong *et al.*, 1966; Greaves, 1983). Aluminous maghemites are commonly found in surface soils that have previously been subjected to burning (Ketterings *et al.*, 2000; Anand and Gilkes, 1987). Al-maghemites are

* E-mail address of corresponding author:
batistamar@hotmail.com
DOI: 10.1346/CCMN.2010.0580401

also found in many tropical soils derived from basic igneous rocks (Costa *et al.*, 1999). In such cases, maghemite is probably produced by aerial oxidation of lithogenic magnetite through a topotactic process (Resende *et al.*, 1986), but the chemical mechanism by which Al^{3+} is incorporated into the spinel structure has not yet been explained well.

The upper limit to isomorphic substitution of Al for Fe in maghemite is also under discussion. Fontes and Weed (1991), for example, reported 16 to 26 mol % Al substitution in maghemites extracted from 12 highly weathered soils of Minas Gerais, Brazil. Under laboratory conditions, the amount of Al that can replace Fe seems to depend strongly on the synthesis procedure. Gillot and Rousset (1990) reported up to 66 mol % Al in maghemites prepared from organic precursors, whereas Wolska and Schwertmann (1989) proposed a limit of 10 mol % for samples prepared from inorganic precursors.

The objectives of the present study were to re-evaluate the extent of Al-for-Fe substitution within synthetic maghemites and to obtain a better understanding of the effect of Al substitution on the structural, chemical, and physical properties of this mineral.

MATERIALS AND METHODS

Synthesis

Aluminous maghemites were prepared by the oxidation of Al-magnetites, synthesized by co-precipitation in alkaline KNO_3 solutions containing $FeSO_4 \cdot 7H_2O$ with stoichiometric amounts of $Al_2(SO_4)_3 \cdot 7H_2O$, according to the procedure described by Schwertmann and Cornell (1991), with the intention to produce isomorphic substitutions of Al for Fe of 0.0, 1.3, 2.5, 3.8, 5.0, 7.5, 10.0, 15.0, 20.0, and 30.0 (1 h equilibration) and 0.0, 5.0, 10.0, 15.0, 20.0, 25.0, 30.0, 35.0, and 40.0 (2 h equilibration) mol %. Magnetite synthesis was performed in an N_2 atmosphere over either 1 or 2 h periods to assess the impact of equilibration time on Al substitution. Following the oxidation and co-precipitation reactions, a hand magnet easily and completely attracted all the magnetite formed. This material was washed several times with distilled water to remove excess salts. It was frozen using liquid nitrogen, and dried in a lyophilizer. The magnetite was then heated in a furnace at 250ºC for 4 h where it was converted to yellowish red maghemite, which was also attracted by a magnet.

Acid ammonium oxalate (pH 3) extraction

In order to purify the maghemites, poorly crystalline materials were selectively removed by one, 4 h treatment with acid (pH 3.0) ammonium-oxalate (2.0 M) in the dark using a sample to solution ratio of 1:1000, according to the procedure described by McKeague and Day (1966). Samples of ~100 mg were weighed into 15 mL polypropylene tubes, and 10 mL of oxalate solution was added. The tubes were capped, covered with Al foil to prevent exposure to light, and shaken in a horizontal shaker for 4 h. After shaking, the suspensions were centrifuged and the supernatants collected for chemical analysis of Fe and A1. Following the extraction, solid residues were washed thoroughly with distilled water to remove excess salts and were then freeze dried for subsequent characterization.

Total chemical analysis

Duplicates of the powdered, purified materials (~200 mg) were weighed into 50 mL polypropylene tubes; 3 mL of concentrated HCl was then added and the samples were allowed to rest for ~48 h until complete dissolution was achieved. The total Al and Fe contents were determined subsequently using inductively coupled plasma mass spectrometry (ICP-MS) using a Varian Vista-MPX ICP-OES instrument. Expected and observed Al and Fe contents were calculated based on the amounts of Al and Fe used in the synthesis and the values obtained in the total chemical analysis, respectively.

X-ray diffraction (XRD)

The powdered material was analyzed on a Philips PW-3020 diffractometer using CuKα radiation (35 kv, 20 mA) in a step-scanning mode (0.01º2θ/2 s) with ~5% Si added as an internal standard for a more accurate determination of *d* values and line broadening. These patterns were exported to *Jade* 3.1® software to determine the areas, heights, positions, and full widths at half maximum (FWHM) of each diffraction peak. The lattice parameter was calculated using a least-squares method solving the general expression for cubic crystals using the Miller indices of 220, 311, 400, 422, 511, and 440 by means of the freeware *UnitCell* (Holland and Redfern, 1997). The mean size of coherently diffracting domains (mean crystallite diameter, MCD) was estimated using the Scherrer formula (Klug and Alexander, 1974); instrumental broadening was assessed from the internal silicon standard.

Specific surface area (SSA)

The specific surface area (SSA_{BET}) was measured by single-point N_2-BET adsorption (Brunauer *et al.*, 1938) using a Micromeritics FlowSorb II 2300 instrument. The specific surface areas were also calculated using the MCD values from the (220) plane of the crystal structure, acknowledging that the crystal is a cubic phase and assuming that the density of the minerals did not change with IS (4.87 g cm^{-3}) (SSA_{Cal}).

Mass-specific magnetic susceptibility (χ_{LF}) and frequency-dependent mass-specific magnetic susceptibility (χ_{FD})

Mass-specific magnetic susceptibility was determined in samples of the Al-substituted maghemites using a Bartington MS2 magnetic susceptibility system coupled with a MS2B sensor (Dearing, 1994). This dual

frequency meter exposed the sample to a weak alternating magnetic field of ~80 A m^{-1}. The MS2B sensor has both low- (0.47 kHz) and high-frequency settings (4.7 kHz) for the identification of fine-grained paramagnetic or superparamagnetic materials. Powdered samples (10 cm^3) were weighed into 20 cm^3 plastic vials. The volumetric magnetic susceptibility (κ) was measured at both low- and high-frequency settings, and the low-frequency mass susceptibility (χ_{LF}) was calculated as follows (Dearing, 1994): $\chi_{LF} = (10\ \kappa_{LF}/m)$, where m is the mass (g). The presence of superparamagnetic minerals with very small particle size (<0.03 μm) was determined from the difference in κ values measured at low- and high-frequency settings and was expressed as the percentage dual frequency magnetic susceptibility (Dearing, 1994): $\chi_{FD}\ \% = [(\chi_{LF}-\chi_{HF})/\chi_{LF}]100$.

Transmission electron microscopy

Transmission electron micrographs (TEM images) were obtained using a Philips EM-300 transmission electron microscope operated at 80 kV. Samples were prepared by dispersing 0.06 g of each maghemite in 30 mL of distilled water with an ultrasonic probe. A drop of each sample suspension was then air dried on a 200-mesh copper grid coated with polyvinyl formvar. The shadowing angle was 26.5º.

Infrared spectophotometric (FTIR) method

The IR spectra were recorded using a Shimadzu model 8300 FTIR spectrophotometer at a spectral resolution of 4 cm^{-1}; each spectrum was obtained after acquiring 95 scans. About 10 mg of each sample plus 200 mg of KBr were weighed and ground with an agate mortar and pestle until an homogeneous mixture was obtained which was then pressed into disc-shaped pellets. The FTIR spectra from the pellets were recorded over the range 400−4000 cm^{-1} and then analyzed using *Origin*® software (5.0, 2001).

Color

Sample colors were determined using a Minolta CR-300 chromameter equipped with a DP-310 data processor as described by Post *et al.* (1993). Approximately 10 g of air-dried material was placed on weighing paper and tamped flat with a petrographic microscope slide. The chromameter projection tube was placed in contact with the sample and a reading was obtained using the Munsell color scale.

RESULTS AND DISCUSSION

Synthesis and chemical analysis

Maghemites were synthesized with different degrees of isomorphic substitution (IS) of Al for Fe; the IS values observed in the synthesized Al-maghemites were less than expected, however, from the relative masses of Al and Fe in the reaction mixture (Table 1). Regarding the stoichiometry of the solutions used to synthesize the Al-substituted maghemites, the efficiency of Fe replacement by Al in the 1 h and 2 h equilibrations averaged 67 and 75%, respectively. The difference in the Al incorporation in the synthesized maghemites was probably due to, among other factors, the lack of a complete solid Fe-Al solution among maghemites (da Costa, 1995) caused by differences in the atomic radii of Fe^{3+} (0.064 nm) and Al^{3+} (0.053 nm).

Linear regression analysis of the expected *vs.* observed IS values for the Al-maghemites synthesized over 1 h or 2 h (Figure 1) revealed that the maximum IS observed for 1 h of reaction (solid line) was 14.3 mol % Al, whereas a 2 h reaction yielded two linear regions, one between 0 and 30 mol % Al (dashed line) and another between 30 and 40 mol % Al (dotted line). The change in the regression coefficient for the dotted lines may have been due to excess Al in the solution, which formed a poorly crystalline Al phase (not observed by XRD). This phase was indistinguishable from the crystalline phase (Al-substituted maghemite) and was not removed by treatment with acid ammonium oxalate

Table 1. Isomorphic substitution (IS) of Al and formula index (x, in $Fe_{2-x}Al_xO_3$) for Fe (mol % and mol, respectively) in the synthetic maghemites.

IS† expected (±0.1)	IS† observed (±0.1)	x expected (±0.01)	x observed (±0.01)
— mol % —		—— mol ——	
	1 h		
0.0	0.0	0.00	0.00
1.3	0.8	0.03	0.02
2.5	1.8	0.05	0.04
3.8	2.8	0.08	0.06
5.0	3.7	0.10	0.07
7.5	5.3	0.15	0.11
10.0	7.0	0.20	0.14
15.0	9.8	0.30	0.20
20.0	11.9	0.40	0.24
30.0	14.3	0.60	0.29
	2 h		
0.0	0.0	0.00	0.00
5.0	4.3	0.10	0.09
10.0	7.4	0.20	0.15
15.0	10.8	0.30	0.22
20.0	14.1	0.40	0.28
25.0	15.9	0.50	0.32
30.0	19.7‡	0.60	0.39
35.0	27.9‡	0.70	0.56
40.0	35.8‡	0.80	0.72

†IS (mol %) = $\{(Al\%/26.98)/[(Al\%/26.98)+(Fe\%/55.85)]\} \times 100$.
‡IS is overestimated, corresponding to 10.6, 15.8, and 21.3 wt.% Al, respectively.

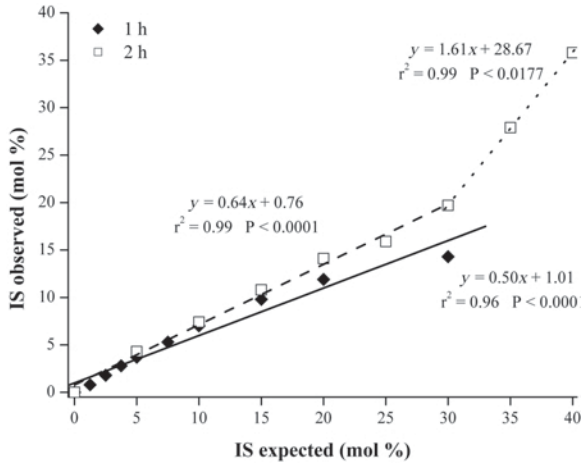

Figure 1. Expected *vs.* observed isomorphic substitution (IS) in synthetic Al-substituted maghemites with 1 and 2 h synthesis times.

at pH 3. The intersection of the dashed and dotted lines suggests that the maximum IS observed in these samples was ~20 mol % Al. The larger regression coefficient (r^2) for the dashed line (first part of the 2 h reaction) relative to the solid line (1 h reaction) indicates that a longer reaction time gives more precision in the isomorphic substitution between expected and observed and greater IS values.

Acid ammonium oxalate pH 3 (AAO) extractions

The Fe_o and Al_o extracted by AAO increased with the total Al content of the samples (Figure 2). The implication is that Al substitution in maghemite decreases the crystallinity and/or increases the surface area (Cornell and Schwertmann, 1996) and thereby enhances reactivity with respect to AAO (Mc-Keague and Day, 1966). Sambatti *et al.* (2002), studying

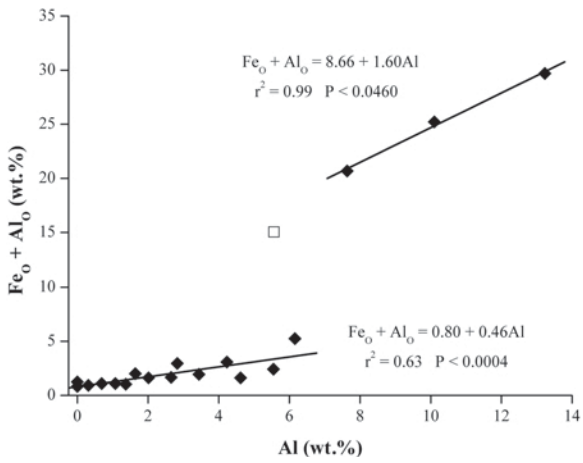

Figure 2. Acid ammonium oxalate (pH 3) extraction of iron (Fe_o) and aluminum (Al_o) from synthetic maghemite samples. (□) Outlier.

synthetic Al-substituted hematites, also observed an increase in the amount of $Fe_o + Al_o$ with increasing IS.

Drastic increases in the $Fe_o + Al_o$ values were observed for Al contents between 6 and 8 wt.%, suggesting that excess Al was not incorporated into the crystal structure of the maghemites but is used up in the formation of a poorly crystalline substance. Therefore, IS calculations from the regression models above this critical value have no meaning because Al was not in the crystalline structure and IS values would be over-estimated.

From Figures 1 and 2, the small IS values were due to the non-incorporation of Al in any mineralogical form, even poorly crystalline materials, *i.e.* under the present working conditions, Al remained in the reaction solution.

X-ray diffraction

Only maghemite and reference Si diffraction peaks were obtained from the AAO-treated samples, indicating that any additional solid phases, if present, were X-ray amorphous or below the detection limit (~3%) (Figure 3). A number of low-intensity diffraction peaks occurred in the pure maghemite specimens. These superstructure lines are weak but clearly visible, indicating an ordered arrangement of the vacancies on B sites (Haneda and Morrish, 1977; da Costa *et al.*, 1994) so that a tetragonal structure can be indexed (Schwertmann and Cornell, 1991). Wolska (1990) also observed a fairly large number of weak superstructure lines in synthetic, Al-substituted maghemites. In the current study, increasing Al-for-Fe substitution eliminated the superstructure lines so that only the six most intense diffraction peaks (220, 311, 400, 422, 511, and 440) were used for further crystallographic characterization. The reduced number of diffraction peaks among the Al-substituted maghemites suggests that incorporation of this metal induced some disorder in the crystals, as observed by da Costa *et al.* (1998). Additional evidence of structural disorder was obtained through decreased peak intensities and increased full width at half maximum (FWHM) values with increasing Al substitution (Figure 3). Progressive increases in FWHM were observed until IS values of 16 mol % Al were achieved (data not given). Above this point, further increases in Al content of the samples induced no detectable changes in peak positions or FWHM and indicated that a limit to Al substitution had been achieved despite the presence of excess Al in both the synthesis solutions and mineral products. Wolska and Schwertmann (1989) also prepared synthetic Al-maghemites from different precursor phases and reported that 10 mol % Al was the maximum substitution.

With increasing Al substitution to 16 mol %, all six indicative peaks (Figure 3) shifted to larger 2θ angles, signaling a progressive decrease in the a_0 unit-cell parameter. This behavior is also demonstrated by the 220 and 311 peaks (Figure 4) and derives from the fact that

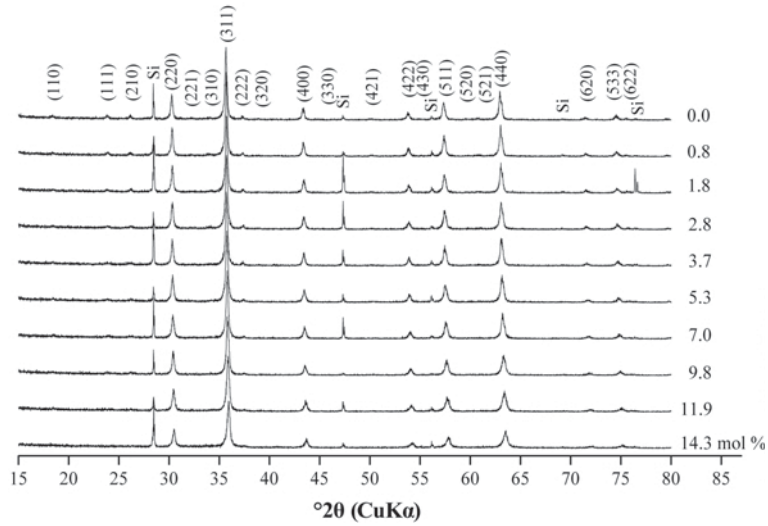

Figure 3. Powder XRD patterns of synthetic, Al-substituted maghemites prepared using a 1 h synthesis time.

Fe^{3+} has a significantly larger ionic radius (r = 0.064 nm) than Al^{3+} (r = 0.053 nm) in octahedral coordination (Kaye and Laby, 1975).

For pure maghemite, the experimental value for a_0 was 0.8339 nm and was close to the value of 0.8351 nm adopted by the Joint Committee on Powder Diffraction Standards (JCPDS card # 39−1.346). The observed relationship between a_0 and the degree of Al substitution was linear and could be described by the following equation: $a_0 = 0.8339 - 396.157 \times 10^{-6}$ Al, which has a correlation coefficient of $r^2 \approx 0.99$ (Figure 5a). The mean crystallite diameter (MCD) of the synthetic Al-substituted maghemites also decreased with increasing IS (Figure 5b) and had a strong positive correlation with the a_0 values (MCD = $7951.4a_0 - 6554.2$, $r^2 = 0.77$).

A similar relationship between a_0 and Al substitution was observed by Schwertmann and Fechter (1984) for a number of synthetic and natural maghemites; the slope for their regression line ($a_0 = 0.8343 - 2.22 \times 10^{-6}$Al), however, was smaller than that observed in this study, and their reported range of Al substitution was 0 to 20 mol %. Fontes and Weed (1991) computed even larger IS

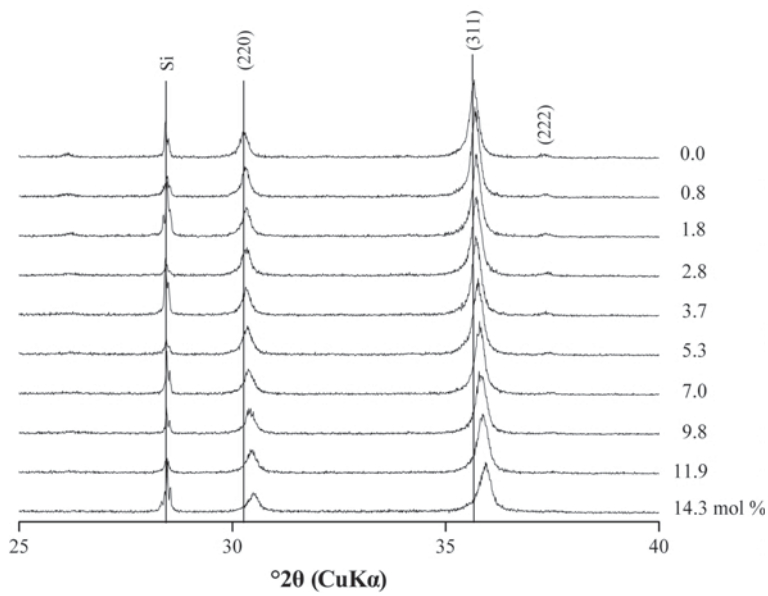

Figure 4. Response of the 311 and 220 diffraction peaks to increasing Al substitution in maghemite prepared using a 1 h synthesis time.

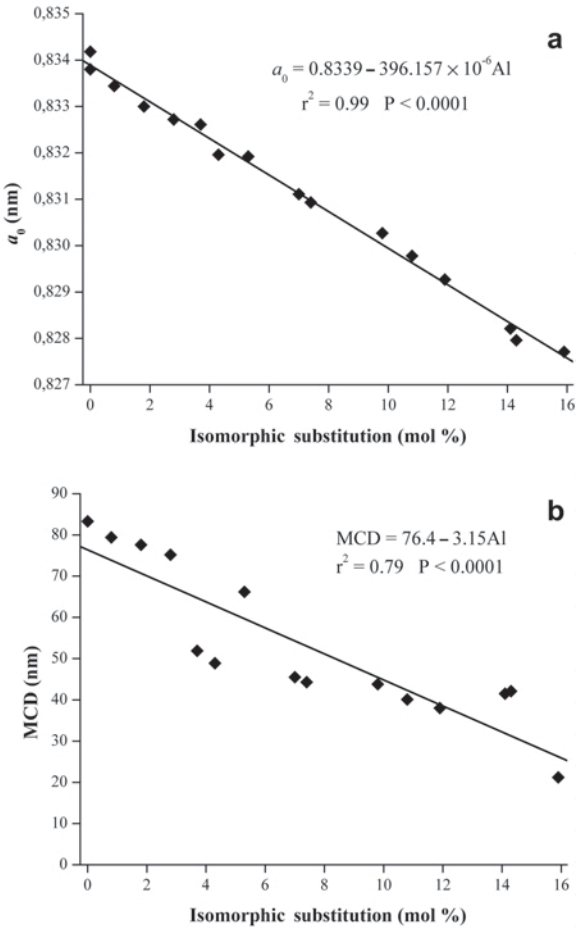

Figure 5. Relations between the IS in synthetic, Al-substituted maghemites and (a) the a_0 unit-cell dimension; (b) the mean crystallite dimension (MCD).

values for soil maghemites (~26 mol % Al) using Schwertmann and Fechter's equation; they noted, however, that the Al content of the natural samples might have been overestimated by the release of some Al^{3+} from kaolinite.

Transmission electronic microscopy

By using TEM, a decrease in the average size of maghemite crystals with increasing Al substitution was observed (Figure 6); the decrease in crystal size was clearly not homogeneous within a given sample, however. The largest crystals (~100 nm) observed at all IS levels were octahedral in shape. Otherwise, the tendency was for the grains to become more subhedral or even anhedral (rounded) with increasing Al content. Although natural and synthetic magnetite are most commonly found as octahedral crystals through the development of the (111) face, magnetites and maghemites formed from other Fe oxides almost always adopt the habit of their precursor (Cornell and Schwertmann, 1996). Taylor and Schwertmann (1974) synthesized maghemites consisting of mostly sub-rounded particles and varying in diameter between 0.02 and 0.06 μm depending on the conditions during synthesis.

Excess Al in the synthesis solution produced a poorly crystalline, X-ray amorphous material that persisted even after AAO extraction. This material can be observed in the samples having 21.3 wt.% Al (Figure 6f).

Specific surface area (SSA)

The relationship between SSA and Al substitution, as well as a comparison of results obtained by the N_2-BET method and those calculated using the MCD of the (220) maghemite diffraction peak, revealed (Figure 7) that the SSA increased linearly with increasing IS, but the slope and intercepts of the regression lines for the two datasets were different. Increases in SSA were expected because the degree of crystallinity and grain size of these samples clearly decreased with increasing IS, as reflected in the aforementioned AAO data (Figure 2), FWHM measurements (Figure 3), and TEM observations (Figure 6). No tendency was observed for the SSA to decline at small values of Al substitution as noted by Schulze and Schwertmann (1987) in aluminous goethites. In that case, SSA values decreased from 52 to 26 $m^2\ g^{-1}$ as the extent of Al substitution increased from 0 to 16 mol %. This effect was attributed to an increase in crystal thickness along the (100) direction together with a reduction in the number of domains per crystal. In synthetic, Al-substituted hematites Schwertmann *et al.* (2000) observed an increase in surface area (BET) with increasing Al content, as observed in the present study.

Results from the direct BET measurements are consistently lower than the indirect XRD measurements for SSA. Similarly, Sidhu (1988) observed that the particle size of maghemite and hematite crystals measured by XRD line broadening were about one-third of those obtained from direct SSA measurements and electron microscopy. The difference between the results might be due to an overestimation of instrumental contributions to the FWHM. Using SSA values obtained by the BET method, the pure maghemite specimens analysed in the present study should have MCD values close to 70 nm.

Mass-specific magnetic susceptibility (χ_{LF}) and frequency-dependent, mass-specific magnetic susceptibility (χ_{FD})

Mass-specific magnetic susceptibility (χ_{LF}) values reported for maghemite (Dearing, 1994) range from 44,000 to $111{,}600 \times 10^{-8}\ m^3\ kg^{-1}$. Costa *et al.* (1999), working with natural maghemites from Brazilian soils, reported an average value of $91{,}000 \times 10^{-8}\ m^3\ kg^{-1}$. As IS increased to 5.3 mol % Al in the current study, χ_{LF} increased from 47,103 to 52,322 $10^{-8} \times m^3\ kg^{-1}$, an 11%

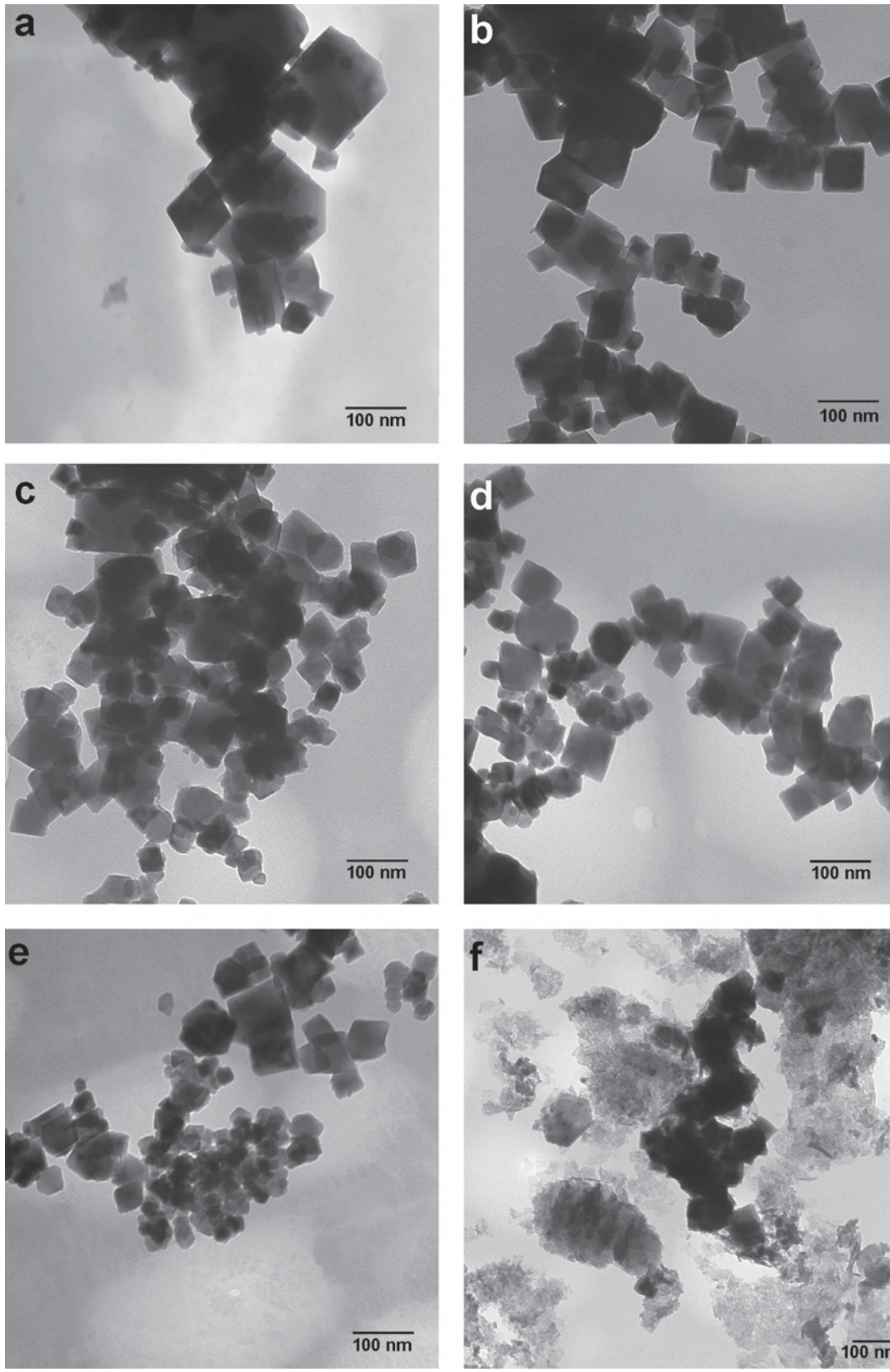

Figure 6. TEM images of synthetic, Al-substituted maghemite, with: (a) 0.0, (b) 1.8, (c) 5.3, (d) 7.4, and (e) 11.9 mol % Al. The sample shown in (f) contains 21.3 wt.% Al.

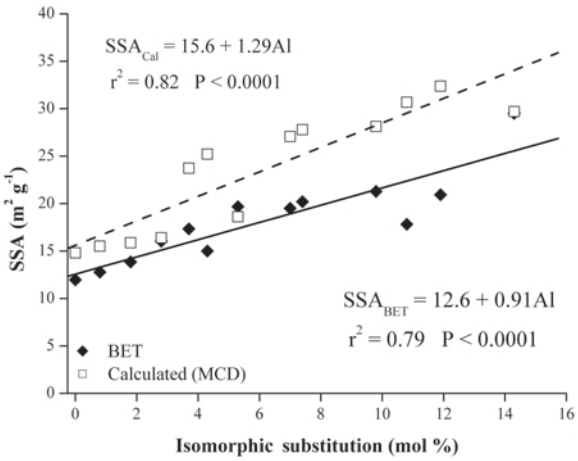

Figure 7. Relation between N_2-BET and MCD specific surface areas (SSA) and mol % Al in synthetic, Al-substituted maghemites.

change (Figure 8). Above this critical value (5.3 mol % Al), χ_{LF} dropped to $31{,}913 \times 10^{-8}$ m^3 kg^{-1} at 14.3 mol Al %, a 39% decrease relative to the maximum χ_{LF} value and a 32% decrease relative to pure maghemite. This behavior was unexpected because Al^{3+} is a paramagnetic ion (Cullity, 1972), and increasing substitution for Fe should yield a steady and linear decrease in the χ_{LF} values as observed by Batista *et al.* (2008) with synthetic Zn-substituted maghemites.

The current behavior may be due to partial relocation of vacancies from octahedral to tetrahedral sites in the structure (Wolska, 1990; Takei and Chiba, 1966). Aluminum ions have been shown to disrupt the ordering of vacancies and to occupy tetrahedral positions in the spinel structure (Gillot *et al.*, 1982). Also reported is that Al substitution in γ-$Fe_{2-x}Al_xO_3$ breaks down the order of both cation and vacancy distributions in the octahedral sub lattice (Gillot *et al.*, 1982). As a result, an overall decrease in magnetization occurs with increasing Al substitution (Wolska, 1990). However, this decrease is not linear. The departure from linearity is possible if some of the Al^{3+} ions and cation vacancies occupy tetrahedral sites in the spinel structure (Gillot *et al.*, 1982). Prasad *et al.* (2005) synthesized and characterized Al-substituted maghemites for medical purposes and observed the same alteration of magnetic behavior, *i.e.* they recorded an increase in the magnetic susceptibility of the maghemites up to 3.5 mol % Al, close to the critical value observed in the present study (5.3 mol % Al).

Maghemites with 7.0, 7.4, 11.9, and 14.3 mol % Al substitution exhibited frequency-dependent characteristics, *i.e.* they had χ_{FD} values $\geqslant$2%. Dearing (1994) suggested that samples with χ_{FD} <2% have virtually no superparamagnetic character or components (<10%) whereas specimens with $\chi_{FD} \geqslant 2\%$ (average) are usually a mixture of multi-domain, single-domain, and superparamagnetic components. These criteria take into account particle size and magnetic behavior when a specimen is exposed to an alternating magnetic field of low and high frequency. The correlation between χ_{FD} with a_0 and MCD was negative according to the equations $a_0 = 0.8333 - 0.0011\ \chi_{FD}$ ($r^2 = 0.82$ $P < 0.0006$) and MCD = $68.85 - 7.490\ \chi_{FD}$ ($r^2 = 0.58$ $P > 0.0365$), demonstrating the strong dependence of magnetization on particle size and supporting the idea that increasing IS reduces the average particle size of the synthetic minerals.

Color

Variations in particle size, morphology, and chemical composition can cause color variations in a particular mineral. The effect of Al substitution on color is especially difficult to quantify because Al substitution influences both particle size and composition. In general, the Munsell hue of goethite becomes redder with increasing Al substitution and yellower with increasing particle size (expressed as MCL_{110}), and the Munsell value falls with increasing Al substitution

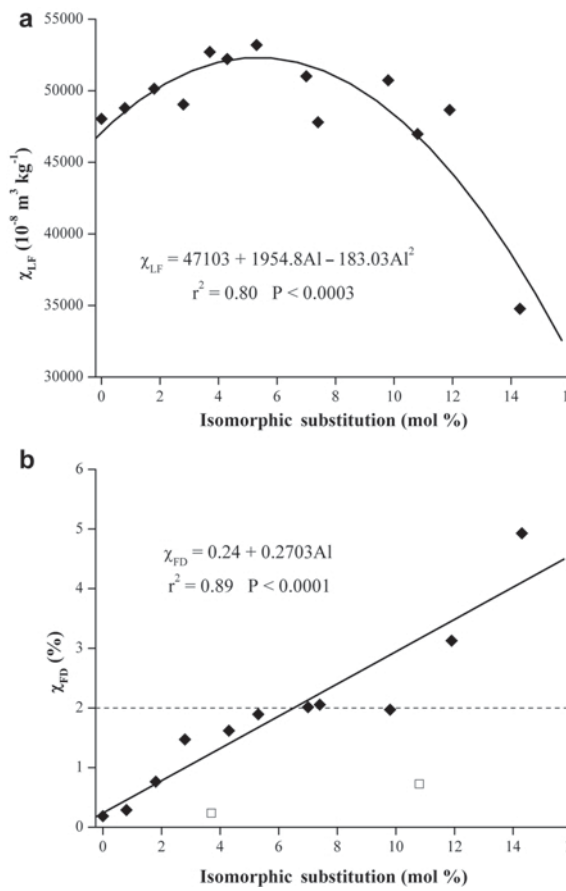

Figure 8. Relations between Al substitution (mol %) in synthetic maghemites and (a) mass-specific magnetic susceptibility (χ_{LF}); (b) frequency-dependent, mass-specific magnetic susceptibility (χ_{FD}). (□) outliers.

(Cornell and Schwertmann, 1996). Structural Al does not appear to significantly influence the hue and chroma of synthetic Al-hematite, although the crystals do become lighter (Munsell value increases) (Barrón and Torrent, 1984; Kosmas *et al.*, 1986).

All maghemites analyzed in this study were yellowish red in color with Munsell hues in the YR range (Table 2), and the samples generally became more yellow with Al substitution. The value and chroma components of the color showed quadratic behavior according to the equations: value = 4.35 − 0.109Al + $0.0073Al^2$ (r^2 = 0.40 P > 0.0814) and chroma = 5.88 − 0.270Al + $0.0176Al^2$ (r^2 = 0.56 P > 0.01687).

Fourier transform infrared spectroscopy (FTIR)

The FTIR spectrum of maghemite included a number of low-frequency bands (800−400 cm^{-1}) that have been assigned to the spinel γ-Fe_2O_3 structure. An interpretation for two of these bands was proposed by Waldron (1955) and White and De Angelis (1967). Specifically, the ν_1 band at 586 cm^{-1} arises from Fe-O deformation in the octahedral and tetrahedral sites while the ν_2 band at 423 cm^{-1} is specific to Fe-O deformation in the octahedral sites. Such bands, with others at 727, 693, 668, 638, 558, 483, and 444 cm^{-1}, are characteristic of well ordered maghemite (Taylor and Schwertmann, 1974).

The FTIR spectra for the series of Al-substituted maghemites (Figure 9) revealed bands at 483, 444, and 423 cm^{-1} in the 0 mol % Al mineral, which changed to a single, broad band at 463 cm^{-1} with 14.3 mol % Al. The features at 727, 693, 638, 586, and 558 cm^{-1} shifted to 738, 705, 650, 597, and 574 cm^{-1}, respectively, with increasing Al content. The band at 668 cm^{-1} was unchanged in all conditions. These results can be correlated directly with the maghemite structure, mainly due to the peaks that shifted to higher frequency indicating an increase in the bond energies. If the observed shifts are not artifacts of the method, then Al substitution introduces significant strain into the octahedral and tetrahedral sites associated with Fe-O vibrations.

Table 2. Color of synthetic Al-substituted maghemites.

IS (mol % Al)	Proportion	Hue	Value	Chroma
0.0	5.4	YR	4.3	6.1
0.8	6.6	YR	4.4	5.8
1.8	6.6	YR	4.1	5.0
2.8	5.5	YR	3.9	4.8
3.7	5.8	YR	4.4	5.7
4.3	6.8	YR	4.1	5.2
5.3	4.8	YR	3.8	4.9
7.0	5.5	YR	3.8	4.6
7.4	6.8	YR	3.9	4.8
9.8	6.6	YR	4.2	5.3
10.8	6.8	YR	3.9	4.9
11.9	6.4	YR	4.2	5.2
14.3	7.1	YR	4.2	5.5

SUMMARY

Maghemites with up to 16 mol % Al were synthesized. The degree of IS in the Al-maghemites was related to the crystallographic a_0 dimension, as given by any one of the six most intense XRD planes (220, 311, 400, 422, 511, and 440), by the linear equation Al (mol %) = $(0.8339 - a_0)/396.157 \times 10^{-6}$. Increasing IS in the maghemite not only resulted in a decrease in a_0, but

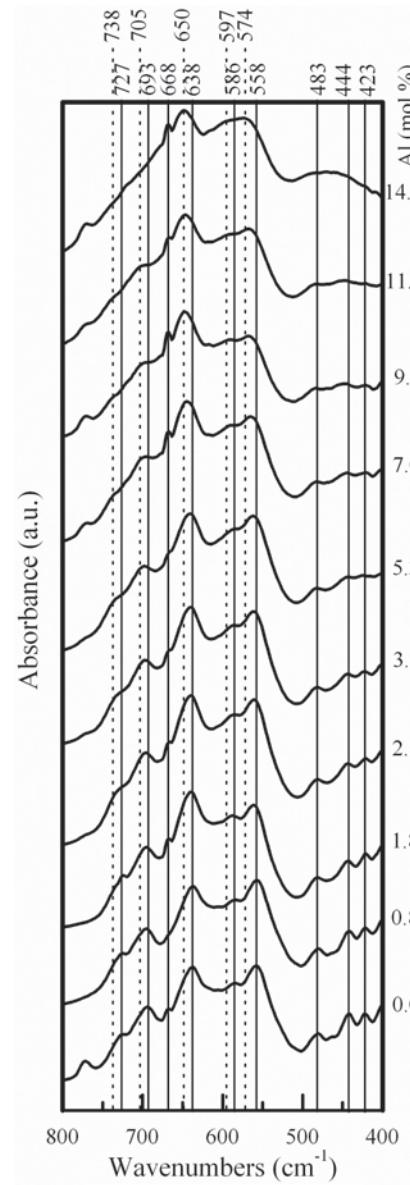

Figure 9. FTIR spectra of synthetic, Al-substituted maghemite in the range 400−800 cm^{-1}.

also in the MCD and degree of crystallinity, whereas the specific surface area and the yellow component of the Munsell hue increased. The effect of structural Al on magnetic susceptibility was positive at small (<5.3 mol %) substitution rates but negative at greater Al contents.

ACKNOWLEDGMENTS

M. A. Batista acknowledges the financial support of CNPq (Conselho Nacional de Desenvolvimento Cientèfico e Tecnológico), under process 140810/2005-6 and 202088/2007-3. The authors thank Mr Franklin S. Jones for his analytical assistance as well as the staff of The School of Environment and Natural Resources, OSU.

REFERENCES

Anand, R.R. and Gilkes, R.J. (1987) Iron oxides in lateritic soils from Western Australia. *European Journal of Soil Science*, **38**, 607–622.

Armstrong, R.J., Morrish, A.H., and Sawatzkya, G.A. (1966) Mössbauer study of ferric ions in the tetrahedral and octahedral sites of a spinel. *Physics Letters*, **23**, 414–416.

Barron, V. and Torrent, J. (1984) Influence of aluminum substitution on the color of synthetic hematites. *Clays and Clay Minerals*, **32**, 157–158.

Batista, M.A., Costa, A.C.S da., Souza Junior, I.G., and Bigham, J.M. (2008) Cristallochemical characterization of synthetic Zn-substituted maghemites (γ-$Fe_{2-x}Zn_xO_3$). *Revista Brasileira de. Ciência do Solo*, **32**, 561–568.

Benjamin, M.M., Hayes, K.F., and Leckie, J.O. (1982) Removal of toxic metals from power-generation waste streams by adsorption and coprecipitation. *Journal of the Water Pollution Control Federation*, **54**, 1472–1481.

Brunauer, S., Emmett, P.H., and Teller, E. (1938) Adsorption of gases in multimolecular layers. *Journal of the American Chemical Society*, **60**, 309–319.

Cabello, E., Morales, M.P., Serna, C.J., Barrón, V., and Torrent, J. (2009) Magnetic enhancement during the crystallization of ferryhydrite at 25 and 50ºC. *Clays and Clay Minerals*, **57**, 46–53.

Campbell, S.J., Kaczmarek, W.A., and Hofmann, M. (2000) Mössbauer insight to metallurgy, materials science and engineering. *Hyperfine Interactions*, **126**, 175–186.

Cornell, R.M. and Schwertmann, U. (1996) *The Iron Oxides: Structure, Properties, Reactions, Occurrence, and Uses.* VCH, Weinheim, New York, Basel, Cambridge, Tokyo.

Costa, A.C.S. da, Bigham, J.M., Rhoton, F.E., and Traina, S.J. (1999) Quantification and characterization of maghemite in soils derived from volcanic rocks in southern Brazil. *Clays and Clay Minerals*, **47**, 466–473.

Cullity, B.D. (1972) *Introduction to Magnetic Materials*. Addison-Wesley, Reading, Massachusetts, USA, 414 pp.

da Costa, G.M. (1995) Mössbauer spectroscopy and X-ray diffraction studies of maghemite (γ-Fe_2O_3) and aluminum-substituted maghemites [γ-$(Fe_{1-y}Al_y)_2O_3$] with $0.0 \leqslant y \leqslant 0.66$. PhD thesis, University of Gent, Belgium, 181 pp.

da Costa, G.M., De Grave, E., Vandenberg, R.E., Bowen, L.H., and de Bakker, P.M.A. (1994) The center shift in the Mössbauer spectra of maghemite and aluminum maghemites. *Clays and Clay Minerals*, **42**, 628–633.

da Costa, G.M., De Grave, E., and Vanderberghe, R.E. (1998) Mössbauer studies of magnetite and Al-substituted maghemites. *Hyperfine Interactions*, **117**, 207–243.

Dearing, J. (1994) *Environmental Magnetic Susceptibility. Using the Bartington MS2 system.* Chi Publications, Kenilworth, UK.

Fontes, M.P.F. and Weed, S.B. (1991) Iron oxides in selected Brazilian Oxisols: I. Mineralogy. *Soil Science Society of America Journal*, **55**, 1143–1149

Gillot, B. and Rousset, A. (1990) On the limit of aluminum substitution in Fe_3O_4 and γ-Fe_2O_3. *Physica Status Solidi. A. Applied Research*, **118**, K5–K8.

Gillot, B., Jemmali, F., and Chassagneux, F. (1982) Availability of Fe ions in Cr- or Al-substituted magnetites with relevance to the process of oxidation in defect phase γ. *Journal of Solid State Chemistry*, **45**, 317–323.

Greaves, C.A. (1983) Powder neutron diffraction investigation of vacancy ordering and covalence in γ-Fe_2O_3. *Journal of Solid State Chemistry*, **49**, 325–333.

Haneda, K and Morrish, A.H. (1977) Vacancy ordering in γ-Fe_2O_3 small particles. *Solid State Communications*, **22**, 779–782.

He, Y.T. and Traina, S.J. (2007) Transformation of magnetite to goethite under alkaline pH conditions. *Clay Minerals*, **42**, 13–19.

Holland, T.J.B. and Redfern, S.A.T. (1997) Unit-cell refinement from powder diffraction data: the use of regression diagnostics. *Mineralogical Magazine*, **61**, 65–77.

Kaye, G.W.C. and Laby, T.H. (1975) *Tables of Physical and Chemical Constants*. Longman, London.

Ketterings, Q.M., Bigham, J.M., and Laperch, V. (2000) Changes in soil mineralogy and texture caused by slash-and-burn fires in Sumatra, Indonesia. *Soil Science Society of America Journal*, **64**, 1108–1117.

Klug, H.P. and Alexander, L.E. (1974) *X-ray Diffraction Procedures for Polycrystalline and Amorphous Materials*, 2nd edition. Wiley, New York.

Kosmas, C.S., Franzmeier, D.P., and Schulze, D.G. (1986) Relationship among derivative spectroscopy, color, crystallite dimensions, and Al substitution of synthetic goethites and hematites. *Clays and Clay Minerals*, **34**, 625–634.

McKeague, J.A. and Day, J.H. (1966) Dithionite- and oxalate-extractable Fe and Al as aids in differentiating various classes of soils. *Canadian Journal of Soil Science*, **46**, 13–22.

Post, D.F., Bryant, R.B., Batchily, A.K., Huete, A.R., Levine, S.J., Mays, M.D., and Escadafal, R. (1993) Correlations between field and laboratory measurements of soil color. Pp. 35–49 in: *Soil Color* (J.M. Bigham and E.J. Ciolkosz, editors). SSSA Special Publication Nº. **31**, Soil Science Society of America, Madison, Wisconsin, USA.

Prasad, N.K., Panda, D., Singh, S., and Bahadur, D. (2005) Preparation of cellulose-based biocompatible suspension of nano-sized γ-$Al_xFe_{2-x}O_3$. *IEEE Transactions on Magnetics*, **41**, 4099–4101.

Resende, M., Coey, J.M.D., and Allan, J. (1986). The magnetic soils of Brazil. *Earth and Planetary Science Letters*, **78**, 322–326.

Sambatti, J.A., Costa, A.C.S. da, Muniz, A.S., Sengik, E., Souza Junior, I. G., and Bigham, J.M. (2002) Relações entre a substituição isomórfica de Fe por Al e as caracterèsticas quèmicas e mineralógicas de hematitas sintéticas. *Revista Brasileira de Ciência do Solo*, **26**, 117–124.

Schulze, D.G. and Schwertmann, U. (1984) The influence of aluminium on iron oxides: X. Properties of Al-substituted goethites. *Clay Minerals*, **19**, 521–539.

Schulze, D.G. and Schwertmann, U. (1987) The influence of aluminium on iron oxides: XIII. Properties of goethites synthesized in 0.3 M KOH at 25ºC. *Clay Minerals*, **22**, 83–92.

Schwertmann, U. and Cornell, R.M. (1991) *Iron Oxides in the Laboratory – Preparation and Characterization*. Verlagsgesellschaft, Weinheim, Germany.

Schwertmann, U. and Fechter, H. (1984) The influence of aluminum on iron oxides. XI. Aluminum-substituted maghemite in soils and its formation. *Soil Science Society of*

America Journal, **48**, 1462–1463.

Schwertmann, U. and Taylor, R.M. (1989) Iron Oxides. Pp. 379–438 in: *Minerals in Soil Environments*, 2nd edition (J.B. Dixon, and S.B. Weed, editors). Soil Science Society of America, Madison, Wisconsin, USA.

Schwertmann, U., Friedl, J., Stanjek, H., and Schulze, D.G. (2000) The effect of Al on Fe oxides. XIX. Formation of Al-substituted hematite from ferrihydrite at 25ºC and pH 4–7. *Clays and Clay Minerals*, **48**, 159–172.

Sidhu, P.S. (1988) Transformation of trace element-substituted maghemite to hematite. *Clays and Clay Minerals*, **36**, 31–38.

Takei, H. and Chiba, S. (1966) Vacancy ordering in an epitaxially grown single crystal of γ-Fe_2O_3. *Journal of the Physical Society of Japan*, **21**, 1255–1263.

Taylor, R.M. and Schwertmann, U. (1974) Maghemite in soils and its origin. II. Maghemite syntheses at ambient temperature and pH 7. *Clay Minerals*, **10**, 299–310.

Waldron, R.D. (1955) Infrared spectra of ferrites. *Physical Review*, **99**, 1727–1735.

White, W.B. and De Angelis, B.A. (1967) Interpretation of the vibrational spectra of spinels. *Spectrochimica Acta*, **23A**, 985–995.

Wiriyakitnateekul, W., Suddhiprakarn, A., Kheoruen-Romne, I., Smirk, M.N., and Gilkes, R.J. (2007) Iron oxides in tropical soils on various parent materials. *Clay Minerals*, **42**, 437–451.

Wolska, E. (1990) Studies on the ordered and disordered aluminium substituted maghemite. *Solid State Ionics*, **44**, 119–123.

Wolska, E. and Schwertmann, U. (1989) The vacancy ordering and distribution of aluminum ions in γ-$(Fe, Al)_2O_3$. *Solid State Ionics*, **32/33**, 214–218.

Zachara, J.M., Ainsworth, C.C., Brown Jr., G.E., Catalano, J.G., McKinley, J.P., Qafoku, O., Smith, S.C., Szecsody, J.E., Traina, S.J., and Warner, A.J. (2004) Chromium speciation and mobility in a high level nuclear waste vadose zone plume. *Geochimica et Cosmochimica Acta*, **68**, 13–30.

(*Received 22 September 2009; revised 26 May 2010; Ms. 362; A.E. J.D. Fabris*)